Received: 21 September 2018 | Revised: 19 November 2018 | Accepted: 21 November 2018
DOI: 10.1002/ppap.201800158

FULL PAPER

PLASMA PROCESSES AND POLYMERS

Superhydrophobic plasma polymerized nanosponge with high oil sorption capacity

Nicolás Torasso[1] | Federico Trupp[1] | Andrés Arias Durán[1,2,3] | Norma D'Accorso[4,5] | Diana Grondona[2,3] | Silvia Goyanes[1]

[1] Universidad de Buenos Aires, Facultad de Ciencias Exactas y Naturales, Departamento de Física, Laboratorio de Polímeros y Materiales Compuestos (LP&MC), Instituto de Física de Buenos Aires (IFIBA-CONICET), Ciudad Universitaria (C1428EHA), Ciudad Autónoma de Buenos Aires, Argentina

[2] CONICET-Universidad de Buenos Aires, Instituto de Física del Plasma (INFIP), Ciudad Universitaria (C1428EHA), Ciudad Autónoma de Buenos Aires, Argentina

[3] Universidad de Buenos Aires, Facultad de Ciencias Exactas y Naturales, Departamento de Física, Buenos Aires, Argentina

[4] Departamento de Química Orgánica, FCEN - UBA, Ciudad Universitaria (C1428EHA), Ciudad Autónoma de Buenos Aires, Argentina

[5] CIHIDECAR-CONICET, Departamento de Química Orgánica, FCEN - UBA, Ciudad Universitaria (C1428EHA), Ciudad Autónoma de Buenos Aires, Argentina

Correspondence
Silvia Goyanes, Universidad de Buenos Aires, Facultad de Ciencias Exactas y Naturales, Departamento de Física, Laboratorio de Polímeros y Materiales Compuestos (LP&MC), Instituto de Física de Buenos Aires (IFIBA-CONICET), Ciudad Universitaria (C1428EHA), Ciudad Autónoma de Buenos Aires, Argentina.
Email: goyanes@df.uba.ar

Funding information
Universidad de Buenos Aires, Grant numbers: UBACYT2014–2017, 20020130100495BA; Ministerio de Educación de la Nación, Grant numbers: RESOL-2016-1233-E-APN-SECPU#ME, 2373/16; CONICET, Grant numbers: PIP 2013-2015 GI 11220120100453, PIP 2014-2016 11220120100508CO

Oil spills in water cause environmental and economic disasters. Herein, a superhydrophobic and oleophilic carbonaceous nanosponge (CN) with high adsorption capacity for selective oil removal from water was developed. It was grown by plasma polymerization of commercial acetylene in a radio frequency glow discharge (RFGD), a single-step, scalable technique. The CN is a porous network of spherical nanoparticles with a broad pore size distribution. It adsorbs 33 times its own weight of light crude oil, with null water adsorption in shaking conditions (ASTM F726-12). Because the CN could be used under sunlight exposure, the effect of UV light irradiation was studied. Potential applications of the CN arise, as it can be deposited on many substrates and change their wetting properties.

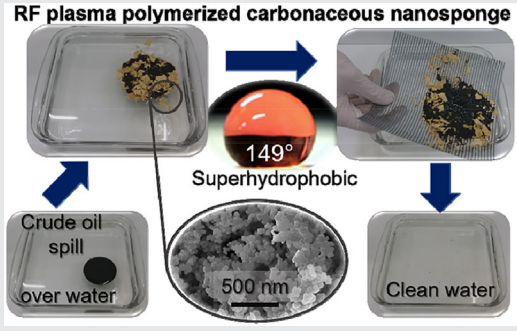

KEYWORDS
hydrocarbons, hydrophobic, nanostructures, oleophilic, RFGD, UV-irradiation

1 | INTRODUCTION

Water is an essential natural component upon which ecosystem functions and all socioeconomic sector depend.[1] In that sense, oil spills on water not only imply adverse environmental impact, but also economic losses in fishing activities, tourism, and petroleum companies.[2] In order to selectively separate oil from water, skimmers and booms are

widespread, but the recovered oil still has 5–10% of water, and the efficiency drops in harsh marine conditions.[3,4] To address this issue, selective sorbents or gelators,[5] pickering emulsions,[6,7] and special wettability membranes[8,9] have been proposed as promising alternatives.

Removal of oil from water through selective sorbents has been studied extensively as it shows several advantages over the other methods, including the possibility of fast recovery of the oil and endurance under harsh marine conditions. Moreover, research on oil spill cleanup using sorbents and nanoparticle technology has shown a continuous growth in the last decade.[10] Different types of carbon materials have been studied as oil sorbents, such as carbon nanotubes, graphene-based sorbents, carbon aerogels, graphite, carbon nanoparticles,[11] active carbon,[12,13] and biochar.[14] Still, two of the great challenges regarding some of these sorbents are a one-step facile production and high sorption capacities.[15,16]

Many studies address the issue of contaminated water by modifying the surface of materials using plasma, but only a few use this technique to fabricate the sorbent.[17] Plasma polymerization is defined as the formation of a material under the influence of plasma, and it has been studied since the sixties.[18] Several mechanisms have been proposed by which carbonaceous materials form during plasma discharges.[19–21] In general, the polymers produced by plasma polymerization do not show a regularly repeated structural unit; in most of the cases they form highly cross-linked and highly branched structures with properties that differ from that of linear polymers synthesized by chemical methods. It is well known that plasma polymerization in a given gas precursor leads to materials with different surface chemical and morphological characteristics depending on the power, working pressure, and geometry of the plasma discharge.[18,22] While low pressure discharges (~0.1 mbar) lead to film structure, higher pressures (~4 mbar) allow the nucleation of nanoparticles (NPs) in gaseous phase, as a consequence of increased collision rate.[23] Some works have even managed to produce carbonaceous-based films or powders in atmospheric plasma dielectric barrier discharges.[24–26] The continuous structure of a film has lower porosity than the discrete particle structure, which implies lower adsorption capacities. Furthermore, a thin film cannot be handled like a powder or any other type of conventional sorbents for oil spills, and for that reason they are restricted to removal of water contaminants in low concentrations. Concerning the case of powder formation in plasma discharges, a critical factor which affects oil adsorption is the size distribution of the nanoparticles, because it determines their stacking and therefore the microstructure of the material.

A carbonaceous absorbent of benzene was obtained by our group in previous work using low pressure plasma technique.[27] It consisted of a thin film of plasma-polymerized acetylene (C_2H_2) deposited on Si substrate by RFGD at low pressure of 0.1 mbar, with a very low base pressure of $\sim 10^{-6}$ mbar. Despite the films prepared in the previous work showed capacity to absorb and retain benzene for the treatment of industrial effluents, they were not hydrophobic (water contact angle of 66°).

By means of a RFGD, Dai et al.[28] obtained porous carbon nanoparticles with diameters between 30 and 50 nm, which were able to selectively absorb silicone oil from a water/silicone oil mixture and organic solvents, such as hexane and toluene, from a water/hexane mixture. This material was obtained using C_2H_2 or a gas mixture of C_2H_2 and CF_4 as the carbon precursors. The authors used a base pressure of $\sim 10^{-5}$ mbar, a discharge working pressure of 0.6 mbar and a source power of 600 W. They showed that it is possible to change the surface energy of the nanoparticles by varying the CF_4 contents in the gas mixture.

It should be noticed that many of the potential uses of oil selective sorbents involve places exposed to sunlight such as water mirrors, open soils, and marine environments. However, most works in the literature do not consider the effect of UV irradiation. Kim et al.[29] prepared a nanosponge by introducing a mix of porous carbon NPs and TiO_2 NPs into a matrix of polydimethylsiloxane. UV activated TiO_2 NPs become hydrophilic and underwater oleophobic, so the nanosponge could release the absorbed oil into water after bubbling and UV exposure. The composite achieves sorbencies of 4.59 g g^{-1} for each cycle and exhibits superoleophilicity in air regardless of the TiO_2 content or UV irradiation.

In this work, a highly hydrophobic with high oil adsorption capacities plasma-polymerized carbonaceous nanosponge (CN) is presented. It consists of a powder-like agglomeration of nanoparticles conforming a porous micrometric structure. The CN was obtained using a capacitively coupled RFGD in commercial grade acetylene at 4 mbar and low power (50 W), with a base pressure of 0.4 mbar. The CN was characterized by SEM, nitrogen porosimetry, thermogravimetric analysis and UV-Vis and FTIR spectroscopies. Oil adsorption and water repellency of the CN were quantified based on ASTM 726-12 "oil adsorption short test" and "dynamic degradation test," respectively, achieving an oil sorbency value of 33 g g^{-1} and no water sorption. Moreover, the effect of UV irradiation over the CN was evaluated. Selective sorption of the CN makes them suitable in various applications, including the areas of water filtration, liquid separation and hydrocarbons spill cleanup.

2 | EXPERIMENTAL SECTION

2.1 | Plasma polymerization and UV irradiation

The reactor employed for the polymerization consisted in a vacuum chamber made of stainless steel with immersed flat

circular electrodes of 28 cm^2 distanced 10 cm apart, as shown in Figure 1. One of the electrodes was connected to the RF power supply (RF VII Inc. 13.56 MHz, 600 W) through a matching unit, and the other electrode was grounded. Plasma-polymerized nanosponges were produced using discharge parameters that guarantee the nucleation of nanoparticles in the plasma phase before reaching the substrate.[30] The chamber was pumped to a base pressure of 0.4 mbar using a rotary vane pump and then filled with acetylene of commercial grade until a working pressure of 4 mbar was reached and held constant. The discharge was turned on for times between 30 s and 10 min with an output RF power of 50 W. The temperature of the substrate was measured with a thermocouple and was held below 50 °C through electrode refrigeration to avoid possible polymer modification by temperature rising. CN was deposited on silicon, aluminum, and glass substrates.

To evaluate UV response of the produced CN, it was irradiated using an UV lamp (Philips HPA 400 s, 400 W) at 75 cm from the sample, which results in a power of 42 W m^{-2}. The UV lamp output spectrum is a rich source of longwave UV-A radiation (315–400 nm), with less contribution from UV-B and UV-C radiations (emission spectrum can be found in Figure S2 of Supporting Information). CN response was evaluated for 0, 15, 30, 63, and 130 min, i.e., energy doses ranging from 0 to 33 J cm^{-2}.

2.2 | Characterization

The surface morphology of the CN was characterized by Field Emission Scanning Electron Microscopy (FE-SEM Zeiss LEO 982 GEMINI) and Transmission Electron Microscopy (TEM, EM 301, Philips). For SEM characterization, the CN was deposited directly on Si substrate and coated with platinum. Images were obtained using electron high tension (EHT) between 3 and 5 kV, and working distances between 1.7 and 4 mm. For TEM characterization, the sample was introduced in ethanol and the CN was dispersed by sonication for 30 min, after which one drop was placed on a Cu grid.

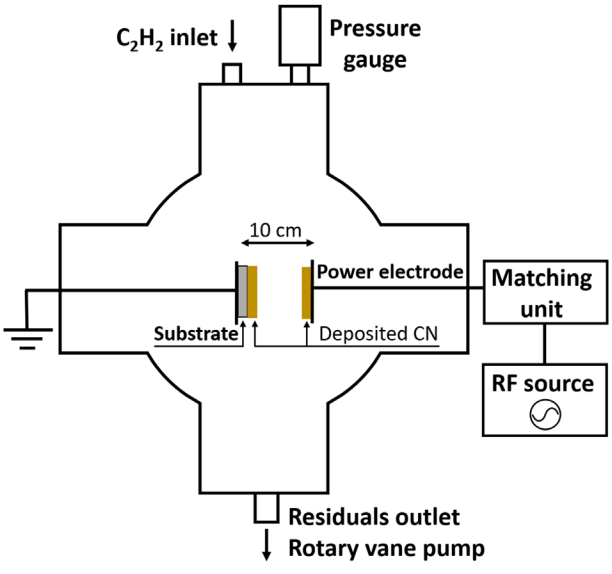

FIGURE 1 RF plasma reactor chamber employed for plasma polymerization

Micromeritics ASAP2020 nitrogen adsorption apparatus (USA) was used to record Brunauer-Emmett-Teller (BET) specific surface area of the CN. All samples were degassed at 100 °C for 24 h before analysis. The pore size distributions were evaluated using desorption data with Barret-Joyner-Halender (BJH) method.

Thermogravimetric analysis of the sample was performed using a Shimadzu DTG-60 under nitrogen atmosphere, with a heating rate of 10 °C min^{-1} and a gas flux of 30 mL min^{-1}.

The infrared spectrum was recorded on a Jasco FTIR 4100 spectrophotometer using the Attenuated Total Reflectance (ATR) mode. UV-Vis spectroscopy was performed with a Shimadzu UV-1800 spectrophotometer in absorbance mode. This study was conducted on the following solution: 10 mg of the CN in 10 mL of tetrahydrofuran (THF), before and after UV exposition. Wetting of the nanosponge deposited on Al substrate for different UV doses was evaluated by contact angle (CA) measurements, which were performed using a USB microscope camera and drops (~20 μL) of distilled water or motor oil Elf Evolution 700 ST 10W40 at ambient temperature. Contact angles were measured with ImageJ software, taken as an average of four measurements for each sample.

Oil adsorption and water take-up of the CN were measured based on the standard procedures in ASTM F726-12 "oil adsorption short test" and "dynamic degradation test," respectively.[31] To determine oil sorbency, a metallic basket of 3 cm^3 and mesh 80 was filled with approximately 65 mg of CN and left to freely submerge for 15 min in crude oil (dynamic viscosity of (23 ± 2) mPa s^{-1} and density (0.88 ± 0.01) g cm^{-3} at room temperature), after which it was lifted and left to drain by the effect of gravity. The weight of the retained oil was measured after 30 s and the sorbency (S) of the CN was calculated as in Equation (1), where W stands for weight.

$$S = \frac{W_{\text{oil sorbed by CN}}}{W_{\text{CN}}} = \frac{W_{\text{retained oil}} - W_{\text{oil adsorbed by basket}}}{W_{\text{CN}}} \quad (1)$$

To determine water take-up of the CN under dynamic conditions, 10 g of the sample were stirred over water for 15 min and left to settle for 2 min. The CN was then picked up with a mesh and weighted. The water pick-up ratio is calculated as the final versus initial weight ratio.

3 | RESULTS AND DISCUSSION

The result of plasma polymerization of acetylene under the conditions detailed in Section 2.1 is a yellow-oranged material which deposits on the electrodes. An image of the CN deposited on the 28 cm^2 grounded electrode after 10 min of plasma polymerization can be seen in Figure 2(a). This material can be recovered from the electrodes and stored in the form of flakes and powder, as shown in Figure 2(b). It is worth to notice that even though the CN was obtained from a small lab reactor, there are commercial and industrial scale RF plasma reactors capable of generating it in larger output, as well as other powder-like polymers.

Figure 2(c and d) shows FE-SEM images in different magnifications of the CN deposited on Si substrate. The nanosponge exhibits a fractal-like, porous structure formed by a network of approximately spherical nanoparticles. As can be seen in the TEM image of Figure 2(e), the CN is effectively composed by an agglomeration of individual nanoparticles, separated for this study by dispersion in ethanol, and with diameters between 8 and 200 nm.

In order to see the growth of the CN for different times, the material was deposited on Si substrate during 30 s, 1 min, and 5 min. SEM images of the respective cross sections is shown in Figure 3. Longer lasting plasma discharges showed an increase in the nanosponge thickness, while maintaining the size distribution of the particles. The deposition rate of the CN was approximately 0.9 μg cm^{-2} s^{-1}.

From the images shown in Figure 3, it can be seen that the structure of the CN is highly porous. It is in fact an agglomeration of nanoparticles forming a microsized structure resembling a sponge with micro and mesopores, but with no elasticity. A quantification of the pore size distribution, obtained by porosimetry, is shown in Figure 4. The CN has a high specific surface area between 141 and 173 m^2 g^{-1}. It is mainly mesoporous and microporous, with contributions to total pore area of 74 and 25%, respectively.

Figure 5 shows the wetting behavior of the CN. It is highly hydrophobic and oleophilic, yielding a water contact angle of $(149 \pm 3)°$ and oil contact angle of practically 0°. These qualities enable the CN to be a selective sorbent. As it is known, contact angle depends on the surface morphology as well as the molecular interactions of the materials. The fractal-like structure of the CN presents high rugosity and porosity which allows the trapping of air inside the particle networks. This is critical to enable the droplet to be in a Cassie-state showing the almost super-hydrophobic behavior of the CN. By the same token, the surface nano-porous structure of the CN, in addition to its molecular affinity to oils, allow the complete wetting Wenzel-state of the oil droplet.

The thermal degradation behavior of the CN was measured in a nitrogen atmosphere. Thermal stability is of importance regarding its potential applications. Results show that the material is thermally stable until approximately 350 °C, temperature at which it starts to degrade (Figure S2 in Supporting Information). For any application at ambient

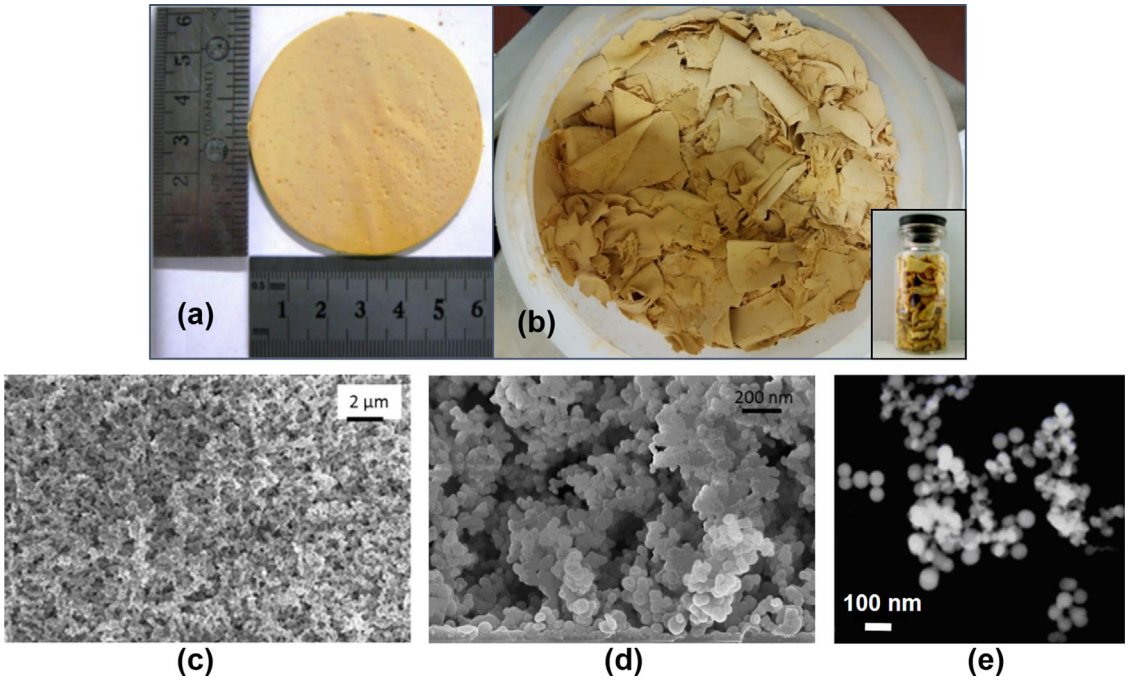

FIGURE 2 (a) Substrate of 28 cm^2 covered by CN after 10 min of plasma polymerization. (b) Stored CN extracted from the electrodes. (c and d) FE-SEM (e) and TEM micrographs of the obtained CN

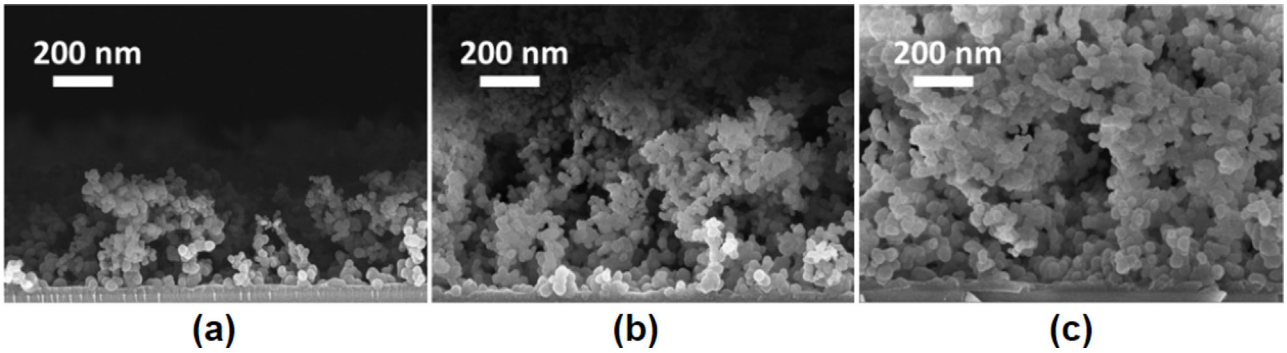

FIGURE 3 SEM images of the CN depositions for different discharge durations: (a) 30 s, (b) 1 min, (c) 5 min

temperature even in sun exposed outdoor environment, the CN will maintain stable. Further, if incineration was desirable after the usage, the study shows that for a nitrogen atmosphere, 500 °C are enough to reduce the mass of the CN more than a 50%. For a complete carbonization, temperatures superior to 700 °C would be needed.

In order to quantify oil sorbency, crude oil adsorption test on the CN was performed and resulted in $(33 \pm 2)\ g\ g^{-1}$. Oil sorbency value of a sorbent is critically affected by the experimental procedure and ambient conditions, as well as by the oil viscosity and density. However, no uniform standard sorbent testing procedure is used by the majority of the scientific community.[32] In this work, ASTM 726-12 procedures have been used, and therefore it is reasonable to compare to other works that use it too. Table 1 shows the oil sorbency (for the "oil sorption short test" of the aforementioned standard test method) of other type II sorbents, which according to the ASTM 726-12 are unconsolidated particulate materials without sufficient form or strength to be handled except with scoops and similar equipment. It can be seen that CN has a relatively high value compared to similar sorbents reported in literature. An example of the removal capacity of the CN is shown in Figure 6. Crude oil spilled over water (Figure 6(a)) can be selectively adsorbed by spreading a certain amount over the oil (Figure 6 (b)) and then lifting the congealed material with a plastic mesh (Figure 6(c)) with pores of approximately 2 mm^2 which allows the drainage of clean, non-adsorbed water back into the recipient (Figure 6 (d)). If a sufficient quantity of CN (sorbency test result suggests that more than 1/33 of the spilled oil mass) is efficiently spread over the oil, it is possible to completely adsorb and mechanically remove it from the water surface until it is no longer visible to the naked eye. Supporting Information Video S3 shows that the CN completely adsorbs crude oil spilled over water in less than 3 min. The fast sorption rate is caused by the capillarity resulting from the nanoporous structure and molecular affinity to oils. No water uptake of the CN could be observed in the dynamic degradation test.

It should be noted that the obtained polymer has a powder or flakes structure, and that it may be thought as a nanosponge because of its porous structure and sorption properties. However, it does not have an elastic, macroscopic defined shape. For this reason, even though some of the sorbed oil may be recovered by the application of pressure over the CN,

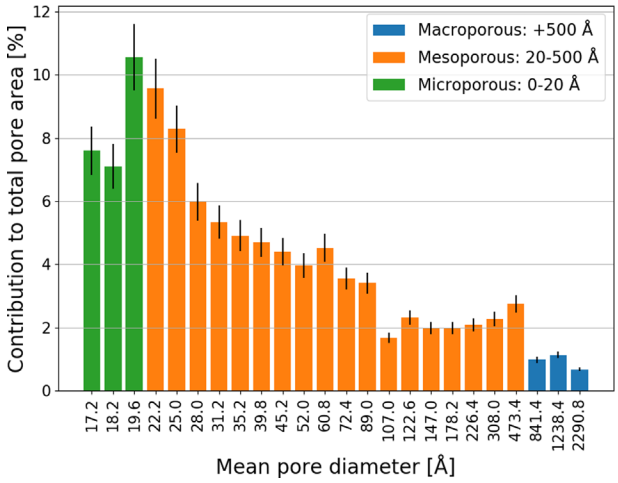

FIGURE 4 Pore size distribution of the CN obtained using BJH method on isothermal nitrogen adsorption-desorption curves

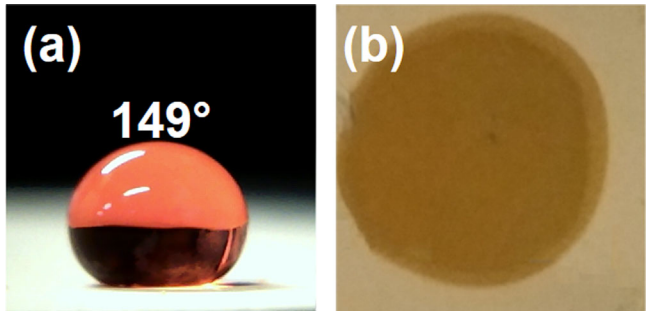

FIGURE 5 (a) Water contact angle of the CN. The water droplet was dyed red. (b) Oil contact angle of the CN

TABLE 1 Type II sorbents for oil recovery tested with the ASTM 726-12 procedures

Material	Fluids	Dynamic viscosity[a] (cP)	Density ($g\,cm^{-3}$)	Sorbency ($g\,g^{-1}$)	Ref.
Natural clay, pillared clay and algae modified clay	Crude oil	–	–	1.61–2.58	[33]
Bagasse	Light crude oil	–	0.873	4.32	[34]
	Medium crude oil		0.916	5.72	
Peat, bagasse, water lily	Diesel oil	3.9	0.828	3.4–4.6	[35]
	Crude oil	15	0.892	4.9–5.9	
	Motor oil	300	0.875	4–5.9	
Lignite fly ash, sawdust	Heating oil	2.68	0.82	1.5–1.7	[36]
	Crude oil	12.04	0.87	2–2.9	
Paper waste: bark, sawdust, belt filter waste and rejects	Diesel oil	4.5	0.8287	9.67	[37]
	Motor oil 0 W40	53 (40°)	0.856	12.84	
	Motor oil 10 W40	70 (40°)	0.880	12.92	
Carbonaceous nanosponge (present work)	Crude oil	23	0.88	33	

[a]Values for temperature used in the test, unless stated.

reusability has not been tested. The CN, like other powder sorbents such as diatomaceous earth, is not intended to be reusable. Final disposition of the CN could be incineration due to its degradation temperature (see TGA in Figure S2).

As stated earlier, the response of the material to UV irradiation is of importance when considering it as an oil selective sorbent in sunlight exposed environments. Figure 7 shows the water and motor oil contact angles of the CN as a function of UV dose on samples of less than 200 μm thick. There is a gradual diminish of the hydrophobicity of the material, until a complete wetting regime is reached (CA of ~0°). Without UV radiation, the water drops are in a Cassie-Baxter regime. Increasing UV dose enhances hydrophilicity until the wetting condition turns to the full wetting Wenzel state. In contrast to water response, oil drops fully wet the surface (CA ~0°) independently of the UV exposure time, showing the unchanged oleophilicity of the CN. A similar response to UV was obtained by Kim et al.,[29] but with a material consisting of a polydimethylsiloxane matrix covered with plasma-synthesized hydrocarbon nanoparticles.

Figure 8 shows ATR-FTIR transmittance spectra of CN deposited on Al substrates and exposed to UV radiation for different times. The broad band around 3300 cm^{-1} corresponds to the simultaneous presence of free −OH groups (3580–3670 cm^{-1}), intermolecular interactions between dimers and trimers (3550–3220 cm^{-1}) and extended interactions of hydrogen bonds (multimers) between 3300 and 3400 cm^{-1}.[38] In this region, UV exposure time produce an increment in hydrogen bond interactions and in the band around 3250 cm^{-1}. The last one is associated to vibrations of hydroxyl groups belonging to carboxylic acids and reveals an increment of these groups with exposure time. This statement is further confirmed by a growing peak around 1720 cm^{-1} due to carbonyl group stretching vibration of carboxylic acids. The appearance of carbonyl groups after UV exposure of the CN was further confirmed by UV-vis spectroscopy. Details of

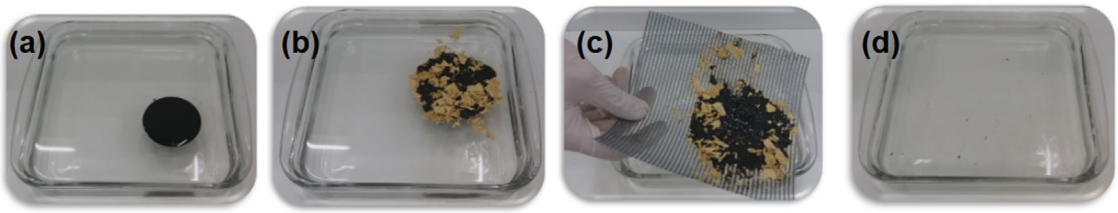

FIGURE 6 Demonstration of crude oil adsorption: (a) crude oil spilled over water; (b) CN spread over the slick; (c) removal of soaked CN with a mesh; (d) clean water after the process

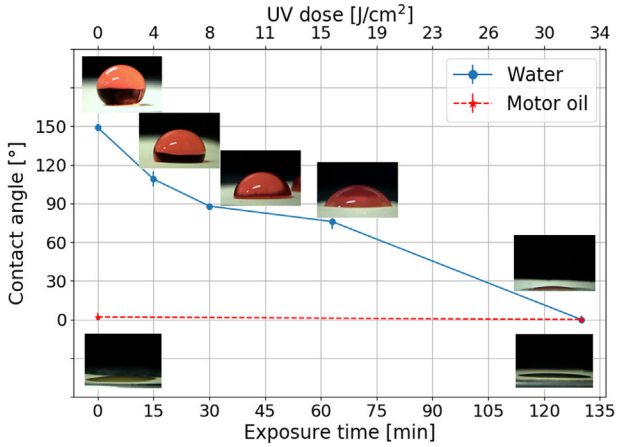

FIGURE 7 Water and motor oil contact angles of the CN for different doses of UV irradiation

this measurement can be seen in Figure S4 of the Supporting Information.

The increment in oxygen content as a consequence of UV irradiation is also detected in the band associated to symmetric stretching vibrations of C–O, around 1220 cm^{-1}.[39]

As could be observed, the appearance of new oxygen bands is a consequence of the photochemical oxidation produced by UV irradiation of the CN, which increments polar groups such as carbonyl and hydroxyl. These molecular changes in the surface of the polymer generate an increment in surface energy, which results in the decrease in the contact angle, observed in Figure 7. No noticeable surface structure modifications were observed in SEM images of the UV-exposed CN (Figure S5 in Supporting Information).

The presence of hydroxyl groups in non-exposed CN can be attributed to the acetone in which the commercial grade acetylene used as precursor gas is stored. Another possible

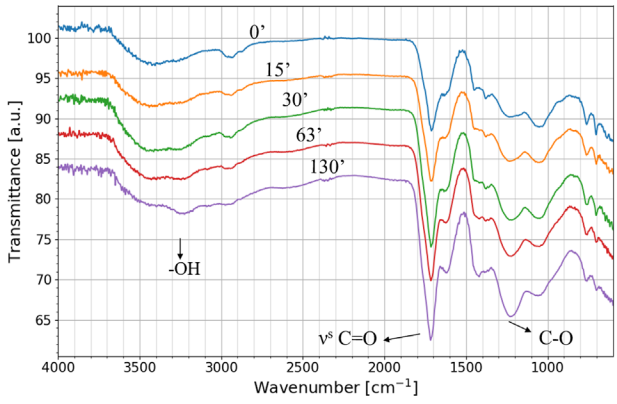

FIGURE 8 ATR-FTIR transmittance spectra of the CN deposited on Al substrate, before and after different times of UV irradiation exposure

mechanism from which a plasma polymerized material may exhibit hydroxyl groups is by the reaction of trapped free radicals with molecular oxygen and water present in air. These trapped free radicals are common in plasma-polymerized species during their production process and their presence has been reported in low pressure plasma polymerization of acetylene.[40]

According to Diffey,[41] the power of UV irradiation coming from sunlight at noon during the summer in northern Europe over an unshaded horizontal surface is 40 W m^{-2}, which is approximately the power flux used in our experiment. Consequently, the times of exposure in this experiment have approximately a one to one correlation to time exposed to sunlight in the conditions stated above. In this sense and considering the sorption rate of the CN (see Supporting Information Video S3), 30 min of UV exposure is much more than the time it would take the CN to act as an oil sorbent in a marine environment. After the first few minutes in contact with the oil, the CN is completely soaked by it. As shown in Figure 7, the UV-exposed CN remains oleophilic. Therefore, even if the UV irradiation continues, the CN does not release the oil it has adsorbed. This means that although the molecular changes shown in the FTIR spectra signify a change in the water wettability of the CN (as shown in Figure 8) the oil-covered CN would not adsorb water (it would have to previously release the oil). In addition, the UV response of the CN was measured in a sample of less than 200 μm thick, while the quantity used in an oil spill would result in a much bigger thickness. Thus, as it is well known that UV irradiation has superficial incidence on polymers, its effect on the overall performance of the CN would be attenuated.

4 | CONCLUSION

An acetylene plasma obtained under low power and low pressures in a potentially scalable process led to a nanoporous material (CN) showing both superhydrophobicity and oleophilicity. The CN can be used to selectively and efficiently adsorb hydrocarbons from water, with negligible water uptake. The material maintains its hydrophobicity for 30 min of UV exposure and it starts wetting afterwards but keeps oil affinity. The change in wetting behavior would not affect the performance of the CN in sunlight exposed environments, considering that its oil sorption rate is enough for it to recover the oil much faster than the time it takes UV irradiation to make the CN hydrophilic.

Due to its versatile deposition, the CN could be used for surface treatment of textiles or metal meshes, producing membranes with potential applications as selective barriers for oil/water separation.

ACKNOWLEDGMENTS

This work was supported by grants from Universidad de Buenos Aires, UBA (UBACYT2014–2017, 20020130100495BA), Ministerio de Educación de la Nación (Secretaría de Políticas Universitarias under the program "Universidades Agregando Valor," awarded by RESOL-2016-1233-E-APN-SECPU#ME, Resolución SPU No. 2373/16) and CONICET (PIP 2013–2015 GI 11220120100453, PIP 2014–2016 11220120100508CO). We thank Y-TEC YPF Tecnología for the crude oil supplied.

ORCID

Silvia Goyanes http://orcid.org/0000-0002-2200-0576

REFERENCES

[1] D. Wu, L. Fang, Y. Qin, W. Wu, C. Mao, H. Zhu, *Mar. Pollut. Bull.* **2014**, *84*, 263.
[2] J. Beyer, H. C. Trannum, T. Bakke, P. V. Hodson, T. K. Collier, *Mar. Pollut. Bull.* **2016**, *110*, 28.
[3] M. Fingas, *The Basics of Oil Spill Cleanup*, 3rd ed., CRC Press, Boca Raton **2013**.
[4] A. E. Ghaly, D. Dave, *Am. J. Environ. Sci.* **2011**, *7*, 423.
[5] F. L. Motta, S. R. Stoyanov, J. B. P. Soares, *Chemosphere* **2018**, *194*, 837.
[6] X. Wang, Y. Shi, R. W. Graff, D. Lee, H. Gao, *Polymer* **2015**, *72*, 361.
[7] A. V. Dudchenko, J. Rolf, L. Shi, L. Olivas, W. Duan, D. Jassby, *ACS Nano* **2015**, *9*, 9930.
[8] M. Padaki, R. Surya Murali, M. S. Abdullah, N. Misdan, A. Moslehyani, M. A. Kassim, N. Hilal, A. F. Ismail, *Desalination* **2015**, *357*, 197.
[9] Z. Dang, L. Liu, Y. Li, Y. Xiang, G. Guo, *ACS Appl. Mater. Interfaces* **2016**, *8*, 31281.
[10] B. Doshi, M. Sillanpää, S. Kalliola, *Water Res.* **2018**, *135*, 262.
[11] S. Gupta, N.-H. Tai, *J. Mater. Chem. A* **2016**, *4*, 1550.
[12] E. A. Emam, *Am. J. Environ. Prot.* **2013**, *2*, 161.
[13] L. W. Hrubesh, P. R. Coronado, J. H. Satcher, *J. Non. Cryst. Solids* **2001**, *285*, 328.
[14] R. Kandanelli, L. Meesala, J. Kumar, C. S. K. Raju, V. C. R. Peddy, S. Gandham, P. Kumar, *Mar. Pollut. Bull.* **2018**, *128*, 32.
[15] A. Abolghasemi Mahani, S. Motahari, A. Mohebbi, *Mar. Pollut. Bull.* **2018**, *129*, 438.
[16] J. Wang, H. Wang, G. Geng, *Mar. Pollut. Bull.* **2018**, *127*, 108.
[17] S. Duan, X. Liu, Y. Wang, Y. Meng, A. Alsaedi, T. Hayat, J. Li, *Plasma Process. Polym.* **2017**, *14*, 1600218.
[18] H. Yasuda, *Plasma Polymerization*. Academic Press Inc., Orlando **1985**.
[19] K. De Bleecker, A. Bogaerts, W. Goedheer, *Appl. Phys. Lett.* **2006**, *88*, 3.
[20] E. Kovacevic, J. Berndt, T. Strunskus, L. Boufendi, *J. Appl. Phys.* **2012**, *112*, 013303.
[21] J. Winter, J. Berndt, S.-H. Hong, E. Kovačević, I. Stefanović, O. Stepanović, *Plasma Sources Sci. Technol.* **2009**, *18*, 034010.
[22] K. S. Siow, *Plasma Process. Polym.* **2018**, *15*, 1800059.
[23] WO 2014020217 (2014), Universidad Del País Vasco-Euskal Herriko Unibertsitatea and Consejo Nacional De Investigaciones Científicas Y Técnicas, invs.: M. Felisberto, L. Sacco, G. Rubiolo, S. Goyanes, A. Eceiza Mendiguren, G. Kortabarria Alzerreka, I. Mondragon Egaña.
[24] P. Heyse, R. Dams, S. Paulussen, K. Houthoofd, K. Janssen, P. A. Jacobs, B. F. Sels, *Plasma Process. Polym.* **2007**, *4*, 145.
[25] B. Nisol, H. Gagnon, S. Lerouge, M. R. Wertheimer, *Plasma Process. Polym.* **2016**, *13*, 366.
[26] U. Reitz, J. G. H. Salge, R. Schwarz, *Surf. Coat. Technol.* **1993**, *59*, 144.
[27] A. Arias-Durán, L. Giuliani, N. B. D'Accorso, D. Grondona, S. Goyanes, *Surf. Coat. Technol.* **2013**, *216*, 185.
[28] W. Dai, S. J. Kim, W.-K. Seong, S. H. Kim, K.-R. Lee, H.-Y. Kim, M.-W. Moon, *Sci. Rep.* **2013**, *3*, 2524.
[29] D. H. Kim, M. C. Jung, S. H. Cho, S. H. Kim, H. Y. Kim, H. J. Lee, K. H. Oh, M. W. Moon, *Sci. Rep.* **2015**, *5*, 1.
[30] M. V. Felisberto, Síntesis, Confinamiento y Alineación de Nanotubos de Carbono: Aplicación a Nanocompuestos Poliméricos Orientados, *Ph.D. Thesis*, Universidad de Buenos Aires **2016**.
[31] ASTM F726-12, *Standard Test Method for Sorbent Performance of Adsorbents*, **2012**.
[32] A. Bazargan, J. Tan, G. McKay, *J. Test. Eval.* **2015**, *43*, 20140227.
[33] O. Katusich, A. Vallone, H. Blasetti, F. Alassia, S. M. Ríos, K. Sapag, N. Nudelman, *Am. J. Mod. Chem. Eng.* **2016**, *2*, 15.
[34] C. M. Á. Díaz-Díaz, L. Rivas-Trasancos, M. León-Barrios, J. Acosta-Sánchez, *Rev. Cuba. Química* **2018**, *30*, 289.
[35] M. Méndez Tobar, J. A. Machado Soberanes, R. Guerra Sánchez, *Tecnol. Ciencia Educ.* **2012**, *27*, 7.
[36] O. K. Karakasi, A. Moutsatsou, *Waste Manag. Res.* **2013**, *31*, 376.
[37] G. Demirel Bayık, A. Altın, *Mar. Pollut. Bull.* **2017**, *125*, 341.
[38] P. C. Blainey, P. J. Reid, *Spectrochim. Acta – Part A Mol. Biomol. Spectrosc.* **2001**, *57*, 2763.
[39] G. Socrates, *Infrared and Raman Characteristic Group Frequencies*, 3rd ed., John Wiley & Sons, Chichester **2004**.
[40] H. Yasuda, T. Hirotsu, *J. Polym. Sci. Polym. Chem. Ed.* **1977**, *15*, 2749.
[41] B. L. Diffey, *J. Cosmet. Dermatol.* **2002**, *1*, 124.

SUPPORTING INFORMATION

Additional supporting information may be found online in the Supporting Information section at the end of the article.

How to cite this article: Torasso N, Trupp F, Arias Durán A, D'Accorso N, Grondona D, Goyanes S. Superhydrophobic plasma polymerized nanosponge with high oil sorption capacity. *Plasma Process Polym.* 2019;16:e1800158. https://doi.org/10.1002/ppap.201800158